Influence of synthetic and bio-based amine curing agents on properties of solventless epoxy varnishes and coatings with carbon nanofillers

Szymon Kugler*, Krzysztof Kowalczyk, Tadeusz Spychaj
West Pomeranian University of Technology in Szczecin, Polymer Institute, Pulaskiego 10, 70-322 Szczecin, Poland
*Corresponding author. Tel. +48 91 449 4833; fax: +48 91 449 4247.
E-mail: skugler@zut.edu.pl

Abstract:
Solventless epoxy varnishes and coatings were prepared using carbon nanotubes (CNT) and/or graphene (GNP) dispersions in a Bisphenol F-type epoxy resin, synthetic [tetraethylenepentamine, poly(oxyethylene)diamine, isophoronediamine, m-xylylenediamine] or bio-based amine hardeners (Cardanol-based phenalkamine; PAA). Room temperature cured coatings, containing 0.35 wt.% of CNT predispersed in PAA, showed outstanding combination of optical (i.e. high gloss and transparency, low haze in humid conditions) and electrostatic dissipative properties (surface resistivity ca. $5.5 \cdot 10^7$ Ω) in relation to the samples containing carbon nanofiller(s) dispersion in the epoxy resin or a synthetic amine. PAA-based coatings with the carbon nanofillers exhibited increased cupping resistance (+20% for samples with CNT) as well as high hardness and excellent adhesion to a glass substrate. The carbon nanofillers addition influenced on curing process and glass transition temperature (monitored using DSC technique) of the epoxy varnishes and coatings as well.

Highlights:
Successful raw carbon nanofiller dispersion in an epoxy hardener (bio-based PAA)
Improved antistatic/optical features and cupping resistance of coatings with PAA/CNT
Proecological solutions: solventless coating system and use of bio-based hardener

Keywords: Epoxy coating; Bio-based amine; Phenalkamine; Carbon nanotubes; Graphene

Graphical abstract:

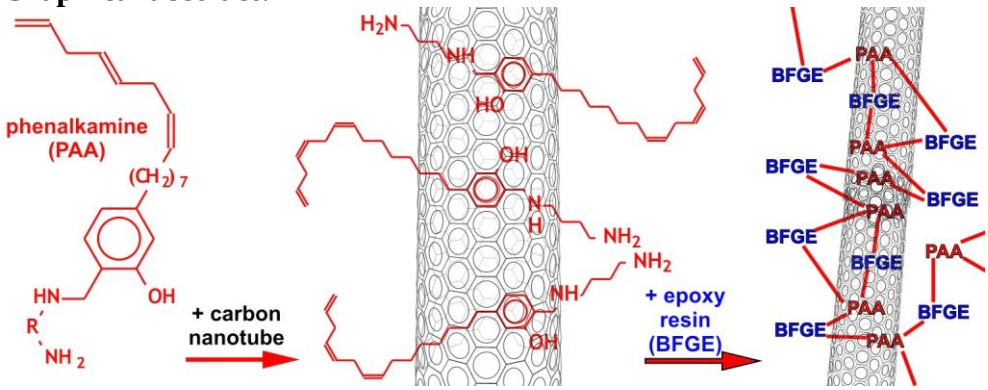

1. Introduction

Nanocomposite polymer films and coatings with recently discovered carbon nanoparticles (CN), i.e. carbon nanotubes (CNT) or graphene (GNP) exhibit many improved properties, such as electrical conductivity [1-11], anticorrosion/ barrier features [5,12-23], thermal stability [6,10,11,14,19,21,22,24-27] , hydrophobicity [11,18,28], adhesion to different substrates [5,13,16,18,20,23,25] as well as mechanical features (i.e. hardness [2,6,10,11,29], tensile strength [4,23,24,30,31], impact strength [14,15,22]). In some cases, higher cupping [15], scratch [7,23,27] and abrasion [13,26] resistance of CN-filled materials are observed as well. Unfortunately, a preparation process of carbon nanofiller-based polymer materials causes several difficulties in practical implementation of these materials, i.e.: (i) obstacles to direct introduction of CN into coating compositions and, (ii) necessity of utilization of toxic/dangerous organic solvents. The former aspect is caused by a lack of chemical affinity between CN and polymeric matrices. The most common way to solve that problem is a surface functionalization of the nanoparticles [32]. Thus, CN for coating applications are

modified by covalent [2,3,9,12,14,16,20-22,26,27,29-31] or non-covalent methods using dispersing agents [1,6,9,11,17,19,24]. Unluckily, covalent methods seriously increase CN price and often negatively influence on features (mainly electrical conductivity [2]) of CN/polymer nanocomposites. Although non-covalent treatment of CN with surfactants [1,19,24,27] or solvents (such as methanol [23], tetrahydrofuran [28] or chloroform [33]) is quite effective and cheap, utilized modifiers (mainly ionic surfactants) may negatively affect on features of nanocomposites and often they are harmful and/or inflammable (solvents). It seems that dispergation of CN in a reactive non-volatile and non-flammable component of a coating system could eliminate the mentioned inconveniences of non-covalent methods. In that situation a commercially available carbon nanofillers could be directly incorporated into a coating system (e.g. 2K epoxy) without their extra functionalization.

It should be noted, that processes of raw carbon nanofillers dispergation in an epoxy resin [25], its solution [5,18,33], or in a whole coating system (based on industrial organic components) [3,4] were utilized and described in the literature. It was revealed that applied epoxy resins (i.e. Bisphenol A/F glycidyl ethers) were indisputable good dispersants for CN [1,2,7,25,29,31], but none of prepared nanocomposite coatings exhibited satisfactory optical properties (while most of unfilled epoxy lacquers create transparent layers). Interestingly, application of raw CN/amine dispersions as components of epoxy coating systems have not yet been discussed in scientific papers. Thus, in this work a series of commercially available synthetic amines with aliphatic, cycloaliphatic and aliphatic-aromatic structures as well as a bio-based long chain aliphatic-aromatic amine (phenalkamine, PAA) were tested as dispersing agents for untreated CNT and GNP. For comparison, dispersions of CN in an epoxy resin were also utilized for preparation of 2K solventless varnishes curable at room temperature. Influence of applied dispersing medium on electrical surface conductivity and transparency of the epoxy coatings (0.35 wt.% of CNT or GNP) were primarily investigated. In the case of PAA-based hardener a few varnishes and coatings with CNT, GNP and CNT/GNP mixture (0-0.35 wt.%) were examined.

2. Experimental

2.1. Materials

Solventless epoxy varnishes were based on the following components:

A) Epoxy components:

- Bisphenol F diglycidyl ether (BFDE), viscosity ca. 3 500 mPa·s (at 25°C), epoxy equivalent weight (EEW) 169 g/eqiv. (Epon 862; Hexion, USA).
- o-Cresyl glycidyl ether (CGE), viscosity 8 mPa·s (25°C), EEW 164 g/eqiv. (EKG; Organika-Sarzyna, Poland).

B) Plasticizer:

- Non-volatile reactive plasticizer (RP) (glycol ester of omega-6 fatty acid), iodine value 150, viscosity 20 mPa·s (25°C) (Archer RC; ADM, USA).

C) Solvent-free amine curing agents (Fig. 1):

- Tetraethylenepentamine (TEPA), amine hydrogen equivalent weight (AHEW) 27 g/eqiv., amine hydrogen functionality (AHF) 7 eqiv./mole, viscosity 80 mPa·s (20°C) (Sigma-Aldrich, Germany).
- Poly(oxyethylene)diamine (JA), AHEW 37 g/eqiv., AHF 4 eqiv./mole, viscosity 798 mPa·s (25°C) (Jeffamine EDR-148; Huntsman, USA).
- Isophoronediamine (IPDA), AHEW 43 g/eqiv., AHF 4 eqiv./mole, viscosity 20 mPa·s (23°C) (Baxxodur EC201; BASF, Germany).
- m-Xylylenediamine (XDA), AHEW 34 g/eqiv., AHF 4 eqiv./mole, viscosity 7 mPa·s (23°C) (Sigma-Aldrich, Germany).
- Cardanol-based phenalkamine (PAA), AHEW 104 g/eqiv., AHF 3 eqiv./mole, iodine value 214, viscosity 650 mPa·s (25°C) (Lite 2002LP; Cardolite, Belgium).

D) Carbon nanofillers:
- Multi-walled carbon nanotubes (CNT), specific surface ca. 275 m^2/g, average length 1.5 μm, average diameter 9.5 nm (NC7000; Nanocyl, Belgium).
- Graphene (GNP), specific surface >750 m^2/g, particle diameter < 0.1 μm and less than 3 carbon layers in a particle (GrapheneX; Graphene Technologies, USA).

2.2. Sample preparation

Epoxy varnishes with CNT and/or GNP were prepared as follows. The carbon nanofiller was introduced to the resinous ("R") component (i.e. BFDE/CGE mixture, 75/25 m/m) or to the hardener ("H") component (amine/RP mixture; 75/25 m/m); system was homogenized for 20 min using ultrasonic homogenizer equipped with ø3 mm sonotrode (UP 200S; Hielscher Ultrasonics, Germany). Coating composition was prepared by mixing (in stoichiometric ratio) of R and H components (unfilled or filled with a carbon nanofiller) for 5 min using a mechanical stirrer. Then, the composition was applied onto glass or steel substrates using a gap applicator and cured for 2 days at room temperature (RT). All samples were additionally kept for 12 days at RT to eliminate potential differences in their crosslinking degree, resulting from use of various hardeners. Composition of the prepared coatings (thickness 30 μm) is presented in Table 1.

2.3. Methods

Viscosity of liquid compositions was evaluated using high shear viscometer (I.C.I. cone-plate system, Research Equipment Ltd, UK). Electrical surface resistivity (ESR) of the prepared coatings (glass substrate, 20°C, 50% RH, 10 V) was determined by means of 6487 electrometer with electrode set 8009 (Keithley, USA). Their transparency (at 700 nm wavelength) was measured using UV-Vis spectrophotometer (V-630; Jasco, USA). Gloss at 20° and haze were determined using Rhopoint IQ206085 device (Rhopoint Instruments, UK) in compliance with the ISO 2813 standard (five measurements of each sample were performed). The surface roughness of coatings (R_a parameter) was assessed using laser scanning microscope VK-9700 (Keyence, USA).
The pendulum hardness of coatings (glass substrate, PN-EN ISO 1522 standard) was tested using König pendulum (AWS-5; Dozafil, Poland). Adhesion to glass substrate was evaluated according to PN-EN ISO 2409 (cross-cut method). Cupping resistance (ISO 1520) of coatings on steel was determined using Model 200 cupping tester (Erichsen, Germany).
Curing process of an epoxy composition was monitored at 25°C (air atmosphere) by means of Differential Scanning Calorimetry (DSC) (Q100 calorimeter; TA Instruments, USA). Glass transition temperatures (T_g) of cured samples were evaluated by DSC as well (20 – 180°C, heating rate of 5°C/min). Thermogravimetric analysis (TGA) was carried out using Q5000 thermoanalyzer (TA Instruments); temperature range was 20–600°C with heating rate of 10°C/min (air atmosphere). Humidity resistance of selected coatings were tested using KBK-100W climate chamber (Wamed, Poland); cured samples were stored for 5 days at 50, 60, 70, 80 or 95% RH (23°C) before tests.

3. Results and discussion

3.1. Coatings containing 0.35 wt.% of a carbon nanofiller and cured with various amines

Table 1 and Fig. 2 A present electrical surface resistivity (ESR) values for epoxy coatings (unfilled or containing 0.35 wt.% of CNT) cured with various amine curing agents. In the case of samples based on the synthetic amines (TEPA, JA, IPDA, XDA) the CNT addition decreased the investigated parameter from $1 \cdot 10^{15}$ Ω (reference samples) to $1.7 \cdot 10^{8}$ - $2 \cdot 10^{9}$ Ω (CNT dispersed in a resinous component; CNT/R) or $7.2 \cdot 10^{11}$ – $1.1 \cdot 10^{14}$ Ω (CNT dispersed in a hardener; CNT/H). It shows that Bisphenol F/cresyl glicydyl ether mixture (aliphatic-aromatic structures) is much more effective dispersing agent for CNT than the aliphatic (TEPA, JA), cycloaliphatic (IPDA) and aliphatic-aromatic (XDA) amines. Interestingly, application of the bio-based long chain aliphatic-aromatic amine (Cardanol-based; PAA, Fig.

1) more significantly reduced ESR of epoxy coatings than above mentioned amines. Moreover, sample based on CNT/PAA dispersions exhibited slightly lower ESR ($5.5 \cdot 10^7$ Ω; E/PAA-C0.35H) than coating prepared using CNT/R dispersion ($9.2 \cdot 10^7$ Ω; E/PAA-C0.35R, Fig. 2 A). Although application of PAA did not highly affect ESR of epoxy coatings modified with graphene (in relation to the samples compounded using synthetic amines), the trend could be noted as well ($8.6 \cdot 10^{13}$ Ω for E/PAA-G0.35H and $8.9 \cdot 10^{13}$ Ω for E/PAA-G0.35R; Fig. 2 A)

Nevertheless, in the case of samples containing synthetic amines and graphene ESR was higher for systems based on GNP/H dispersion than GNP/R component (Table 1 and Fig. 3A). Generally, higher ESR of GNP-filled coating materials (in comparison with the samples containing CNT) was heretofore reported by authors [6] and others [2]. It is known that single GNP particle reaches higher electrical conductivity than multi-wall carbon nanotube, but that parameter value is significantly higher for compressed CNT than GNP powder. A simple explanation of that phenomenon is the presence of numerous contact points between adjacent CNT in a polymer nanocomposite [34]. On the other hand, lower ESR of CN/PAA-based coatings (in relation to all other presented systems) was resulted by better dissipation of a carbon nanofiller in the epoxy matrix due to higher polarity of PAA than BFDE, TEPA, JA, IPDA or XDA. The Cardanol derivative molecule bearings aromatic ring (high affinity to CN structure) as well as one phenolic hydroxyl group and two (i.e. primary and secondary) aliphatic amine groups. Steric stabilization of dispersed CN was achieved by the presence of a long-chain unsaturated substituent in PAA. Probably, thanks to asymmetric localization of the amine groups (at one end of molecule) and OH group presence that hardener does not lose its surfactant-like feature during reactions with an epoxy component. Microphotographs presenting dissipation of carbon nanotubes in the coatings based on IPDA or PAA (0.35 wt.% of CNT) were showed in Fig. 4.

Transparency values for coatings filled with CNT or GNP (0.35 wt.%) are presented in Fig. 2 B or Fig. 3 B, respectively. As can be observed, a type of hardener did not significantly affect transparency of the unfilled samples (ca. 83% at 700 nm), but that parameter was reduced by the nanofiller addition. It should be noted that the mentioned phenomenon was especially visible for CNT-filled coatings based on TEPA, JA or XDA amine (44-50%); the highest transparency values were registered for systems compounded using IPDA (59% for E/IPDA-C0.35R, 69% E/IPDA-C0.35H) or PAA (59% and 66%, respectively). It is noteworthy that CNT dispergation in the resinous component (R) negatively affected the investigated parameter. Considering samples containing 0.35 wt.% of GNP it could be claimed that the coatings based on PAA amine reached higher transparency (73-74%) than samples containing the synthetic amines (65-71%) (Fig. 3).

Applied amine hardener affected gloss of unfilled coatings (Fig. 2 C); high gloss (i.e. >100 gloss units) was noted for the samples based on IPDA (176 G.U.), PAA (159 G.U.) and TEPA (129 G.U.). As can be seen in Figs 2 C and 3 C, addition of the carbon nanofillers (mainly CNT) significantly lowered that parameter value. Coatings with IPDA exhibited 45-82 G.U. (CNT) or 99-112 G.U (GNP) while systems with PAA reached 76-101 G.U. (CNT) or 90-120 G.U. (GNP). Relatively high gloss was also registered for samples containing TEPA and GNP (81-99 G.U., Fig. 3 C). Generally, gloss of coatings modified with CN correlated with their transparency (Figs 2 B and 3 B) and was higher for the samples with GNP and samples based on CN/hardener dispersion (in comparison with the samples containing CNT and/or dispersion of CN in the epoxy component). Considering that CN (mainly CNT) or its agglomerates may protrude from coatings [10], it seems that their gloss values depend on nanofiller dissipation effectiveness in a polymeric matrix. Thus, gloss of tested coatings correlated with their surface roughness, e.g. R_a parameter values for IPDA-based samples were 0.367 μm (45 G.U.; E/IPDA-C0.35R) and 0.196 μm (82 G.U.; E/IPDA-C0.35H) while

sample containing CNT predispersed in PAA reached ca. 0.074 μm (101 G.U.; E/PAA-C0.35H).

It could be claimed that gloss of unfilled coatings depends on reactivity of the varnishes and their tendency to react with carbon dioxide from air. It is known that creation of ammonium carbonate/carbamate results in blushing/blooming of an epoxy coating surface. As presented in [35] that phenomenon has not yet been explained, however, a few approaches to blush elimination have been known. Unfortunately, results of calorimetric analysis (isothermal DSC) of epoxy varnishes curing processes (Table 2) do not correlate with gloss test results of the related coatings. For example, the highest reactivity (i.e. shortest time to 50% conversion of epoxy groups; $t_{\alpha 1/2}$) was noted for medium glossy coating (E/TEPA, 165 min, 129 gloss units) while that parameter value for E/IPDA (the highest gloss; 175 G.U.) was ca. 283 min. Moreover, functionality (AHEW value) of the investigated amines, their viscosity (see Section 2.1) as well as their basicity (e.g. pKa values for TEPA, IPDA and XDA were ca. 4.2 [36], 10.4 [37] and 9.2 [38], respectively) do not correlate with gloss of the samples.

Chemical structure of PAA significantly affects the curing process of unfilled epoxy composition (Table 2). As can be seen, t_{max} parameter value (time to maximum heat flow) for E/PAA sample was lower (49 min) in relation to E/TEPA (70 min) and other R+H neat epoxy systems (131-215 min). Probably, it was caused by Ph-OH group presence in the PAA molecule which accelerates initial addition of epoxy and amine groups; it is generally known that phenol is an active catalysts of that reaction [39]. Nevertheless, due to steric hindrances in a created adduct the further addition reactions are slower. Thus, epoxy group conversion at t_{max} (α_{Hmax}) for E/PAA composition (6%, Table 2) was markedly lower than for other neat epoxy systems (19-55%). On the other hand, 50% conversion of epoxy groups ($t_{\alpha 1/2}$) in E/PAA material was reached in similar time (232 min) as for E/JA (224 min; α_{Hmax}=26%) and E/XDA (213 min; α_{Hmax}=55%).

Considering coating systems with the highest transparency and gloss (IPDA and PAA-based systems; Figs. 2 and 3), it could be observed that CN addition (i.e. nanofiller type and its dispergation method) resulted in changes of their curing process monitored by DSC technique (Fig. 5, Table 2). Incorporation of CNT (0.35 wt.%, mainly as a dispersion in H component) to E/IPDA varnish decreased t_{max} (from 184 min to 99 min), α_{Hmax} (from 34% to 21%) and enthalpy of the process from 309 J/g to 188 J/g. Time $t_{\alpha 1/2}$ was also reduced from 283 min to 234 min (E/IPDA-C0.35R). Interestingly, in the case of PAA-based compositions filled with CNT the α_{Hmax} parameter (epoxy groups conversion at t_{max}) was increased from 6% to 10% (E/PAA-C0.35H) and 14% (E/PAA-C0.35R). Moreover, t_{max} was increased (from 49 min to 57 min) while ΔH_{cure} was lowered from 304 J/g to 143 J/g (E/PAA-C0.35R). The latter parameter was also diminished (179 J/g) after incorporation of GNP in form of dispersion in R component. Epoxy groups conversion at t_{max} was not affected by GNP, but t_{max} was markedly reduced from 49 min to 35 min (GNP/R dispersion) and 23 min (GNP/H).

Considering the fact that enthalpy of a whole curing process cannot be changed and the presented data (Table 2) concern 24-hour curing tests, it could be claimed that crosslinking processes of the CN-filled samples (mainly E/IPDA-type) were slower and longer. In that case, values of α_{Hmax} and $t_{\alpha 1/2}$ should be calculated on the basis of total enthalpy value (ΔH_{cure}) recorded for a reference/unfilled sample; it confirms that CNT addition to IPDA-based coatings significantly reduced epoxy groups conversion (at a heat flow peak) from 34% to 23% (E/IPDA-C0.35R) and 13% (E/IPDA-C0.35H). Interestingly, CNT (predispersed in R component) or GNP (predispersed in R or H component) did not markedly affect α_{Hmax} of E/PAA compositions while CNT/H dispersion increased epoxy groups conversion up to 10% (E/PAA-C0.35H; Tab. 2). It is noteworthy, that curing processes of epoxy compositions filled with CNT were investigated (using DSC technique) and discussed in the literature [40], but the tests were not carried out isothermally at room temperature.

Presented results showed an interaction between CN and varnish components. Generally, carbon nanofiller particles act as physical obstacles for growing polymer chains, but some reactive molecules (with aromatic rings) may be uniquely oriented in the presence of CN and their reactivity may be changed. Probably, it was the reason of higher epoxy groups conversion at t_{max} (α_{Hmax}) of epoxy compositions with PAA and CNT (10%, E/PAA-C0.35H) in relation to the unfilled sample (E/PAA, 6%, Tab. 2.). It should be noted that t_{max} for the samples with 0.35 wt.% of was similar (CNT/H, 49 min) or higher/longer (CNT/R, 57 min) than for the reference sample.

Interestingly, CNT addition influence on glass transition temperature (T_g) of tested materials (Table 1) . As can be seen, coatings filled with the carbon nanofiller exhibited much higher value of that parameter (29°C for the samples based on CNT/R and CNT/H components) in comparison with E/PAA and samples with graphene (22°C). Increment of T_g of polymer materials modified with CNT was recorded by other researches (using DSC [29] as well as Dynamic Mechanical Analysis technique [2,7,8,29]). It is noteworthy that T_g of the other coatings was not so significantly affected by CNT (or GNP) addition (Table 1). Evidently, a relatively low T_g value of PAA-based coatings (in relation to materials with TEPA, JA, IPDA or XDA) was caused by the presence of a long-chain substituent in PAA structure (it acted as a plasticizer of the coatings) and low functionality (i.e. high AHEW and low AHF values) of the bio-based phenalkamine.

The above presented results showed that CN-filled epoxy coatings cured with PAA (especially E/PAA-C0.35H) exhibited better electrical and optical properties than samples with the other hardeners, thus the coating systems based on CN/PAA dispersion were chosen for further tests.

3.2. Coatings containing CNT and/or GNP and cured with PAA amine

Addition of carbon nanofillers increased viscosity of the epoxy varnishes based on PAA hardener (Fig. 6.). As can be seen, CNT influenced this feature much more than GNP; the viscosity value for CNT-modified composition rose up to 500 mPa·s (0.35 wt.% of CNT, E/PAA-C0.35H) while GNP nanofiller increased that parameter to 380 mPa·s (E/PAA-G0.35H). This significant growth of viscosity at relatively low content of CNT (in relation to GNP) can be explained by elongated shape of carbon nanotubes and better GNP dissipation in epoxy composition. It is known that CNT create stranded webs/structures, whereas separated flat particles/aggregates of GNP can be found in a liquid varnish. It should be reminded that cured coatings (E/PAA-type) containing GNP reached relatively lower electrical resistivity as well higher transparency in comparison with CNT-filled samples (Figs. 2 and 3). Considering varnishes containing 0.35 wt.% of CNT/GNP mixture, it could generally be claimed that viscosity of the compositions increased with increasing CNT content in the nanofillers mixture. Nevertheless, it was observed that the varnishes containing 0-0.1 wt.% of CNT (and 0.25-0 wt.% of GNP, respectively) exhibited similar viscosity values, i.e. ca. 380 mPa·s. It should be noted that the investigated parameter value for the varnish containing merely 0.1 wt.% of CNT (E/PAA-C0.1H) was ca. 370 mPa·s (Fig. 6). Interestingly, viscosity (or ESR and transparency; Fig. 7) of the samples containing 0.35 wt.% of CNT/GNP mixture significantly increased (respectively decreased) when the CN mixture contained more than 0.1 wt.% of CNT (< 0.25 wt.% of GNP). Probably, at that weight ratio of tested nanofillers the physical interactions between CNT and GNP particles take place (hybrid carbon matrix is created).

Generally, addition of CNT or CNT/GNP nanofillers to the epoxy varnish (E/PAA) decreased its ESR value up to 8 orders of magnitude; electrostatic dissipative properties (i.e. $<10^{11}$ Ω, [41]) were achieved for coatings with 0.3-0.35 wt.% of CNT and coatings containing CNT/GNP mixture (at least of 0.2 wt.% of CNT: E/PAA-C0.3/G0.05H, E/PAA-C0.25/G0.1H and E/PAA-C0.2/G0.15H). Such significant reduction of ESR was not recorded for samples

containing GNP only. Differences of electrical features of polymer materials filled with CNT or GNP can be found in a literature. Primarily, they were caused by the shapes of CNT and GNP particles; elongated CNT easily form conductive structures in a polymeric matrix in contrast to wrinkled (or aggregated) GNP. Nevertheless, in the CNT/GN mixture (at a proper CNT/GNP ratio) graphene particles act as "electrical switchboards" improving current flow through the modified coating [6]. Fig. 8 shows ESR of nanocomposite coatings investigated by other authors [1,3,6-8,11,42,43]. As can be seen, results for epoxy coatings based on CNT/PAA dispersion were similar or better than for samples achieved from solventless [1,3], solvent-borne [42] and water-borne [6,11] compositions; only special UV-cured coatings [7,8,43] reached lower ESR than the samples with PAA.

The prepared epoxy coatings with carbon nanofillers showed fair transparency (Fig. 7 B). Mentioned parameter decreased with growing content of CN (mainly CNT) in the samples from 84% (unfilled sample, E/PAA) to 66% (E/PAA-C0.35H) and 74% (E/PAA-G0.35H). Transparency of the coatings with CNT/GNP mixtures varied in the range of 66-74% . Moreover, carbon nanofillers addition reduced gloss of the epoxy coatings with PAA from 159 G.U. (unfilled sample) to 101 G.U. (CNT) and 120 G.U. (GNP) (Fig. 7 C). Interestingly, the cured varnishes containing 0.05-0.2 wt.% of CNT (and 0.3-0.15 wt.% of GNP) reached higher gloss than coatings with 0.35 wt.% of CNT or GNP. Summarizing, application of CNT/GNP hybrid nanofiller (0.2/0.15 m/m; total content 0.35 wt.%) allows to prepare the electrostatic dissipative coatings (i.e. ESR $\leq 10^{11}$ Ω) with higher gloss (E/PAA-C0.2/G0.15H, $8.0 \cdot 10^{10}$ Ω, 125 G.U.) than the sample containing 0.3 wt.% of CNT only (E/PAA-C0.3H, $2.1 \cdot 10^{9}$ Ω, 103 G.U.). Nevertheless, the lowest ESR value was achieved for epoxy coating containing solely 0.35 wt.% of carbon nanotubes predispersed in PAA-based hardener ($5.5 \cdot 10^{7}$ Ω, E/PAA-C0.35/H, Tab. 1, Fig. 7 A).

Addition of carbon nanofillers influence on hardness, cupping resistance as well as thermal stability of PAA-based coatings (Table 3). Generally, incorporation of CNT (0.2 or 0.35 wt.%), GNP (0.15 or 0.35 wt.%) or CNT/GNP mixture (0.2/0.15 m/m; 0.35 wt.%) slightly decreased hardness of the cured coatings (from 147 a.u. to 141 a.u., E/PAA-G0.15H), but improved their cupping test results (from 10.0 mm to 12.0 mm; E/PAA-C0.35H). It is noteworthy, that sample containing 0.35 wt.% of CNT exhibited highest values of these parameters in relation to other samples with CN (i.e. GNP or CNT/GNP). Interestingly, Kalendová and coworkers have noted negative influence of a CN on drawability of cured epoxy coatings [15].

Samples with CNT, GNP (0.15 wt.%) or CNT/GNP exhibited lower thermal stability than the reference material; temperature of 10% mass loss (T_{10}) was reduced from 309°C (E/PAA) to 294°C (E/PAA-C0.35H), 300°C (E/PAA-G0.15H) and 301°C (E/PAA-C0.2/G0.15H; Table 3). In the case of sample with the highest graphene content a decrement of T_{10} was not registered (310°C; E/PAA-G0.35H). Considering results for CN-filled materials presented in the literature [6,11] it can be concluded that CNT, GNP and their mixture increase hardness and/or thermal stability of materials based on soft/uncured polymeric matrices only.

The unfilled coating (E/PAA) exhibited excellent adhesion to a glass substrate (Table 3). That parameter was not reduced by CN addition; similar results were presented in the literature [13,20].

Additionally, stability of ESR and optical properties of E/PAA-C0.35H coating was investigated during its exposure in humid conditions (50-95% of RH) (Fig. 9). As can be seen, ESR, gloss, transparency as well as haze (turbidity) of the cured sample were not markedly change during the test. It shows high hydrophobicity of the epoxy coatings cured by Cardanol-based phenalkamine and modified with carbon nanotubes (dissipated in the polymeric matrix without additional dispergation agents).

4. Conclusions

The carbon nanofillers (CN), i.e. nanotubes (CNT) and graphene (GNP) were dispersed in an epoxy resin, as well as in synthetic amine hardeners and bio-based Cardanol derivative (PAA) in order to prepare 2K solventless epoxy coatings. Performed electrical, optical, mechanical and thermal tests showed, that coatings based on CN/PAA dispersions had better properties than materials with CN dispersed in epoxy resin or synthetic amines. This was possible due to high compatibility of CN (especially CNT) and the Cardanol derivative. Generally, the nanocomposite coatings with PAA exhibited lower electrical surface resistivity as well as higher transparency and/or gloss than samples based on aliphatic, cycloaliphatic or aliphatic-aromatic hardener. Although CNT, GNP or CNT/GNP mixture (dispersed in PAA) improved cupping resistance of cured epoxy coatings (+ 2 mm, sample with 0.35 wt.% of CNT), these additives slightly reduced their hardness (e.g. - 6 hardness units, 0.15 or 0.35 wt.% of GNP) and thermal stability (- 17°C, 0.2 wt.% of CNT). Nevertheless, the most important parameters, i.e. electrical surface conductivity, transparency, gloss and haze of cured varnishes (prepared using solely commercially available components, including PAA and CNT) were stable in high humidity conditions. Presented results show that bio-based PAA acts as effective epoxy resin curing agent and dispersing medium for CNT. Due to strong chemical affinity of nanofillers for prepared varnishes, there is no way to separate a nanofiller from such composition, as well as from cured coating, so they are free from potential asbestos-like pathogenicity. Moreover, the absence of flammable volatile components allows to apply these materials in poorly ventilated spaces. Consequently, such transparent (65% of light transmittance) and antistatic coatings ($5.5 \cdot 10^7$ Ω; sample with 0.35 wt.% of CNT predispersed in PAA) can be produced on lampshades or sight-glasses used in explosive atmosphere in mines and chemical installations.

Acknowledgements

This work was financially supported by Polish National Science Centre (project no. 2014/13/N/ST8/00092). Authors thank Cardolite Corporation (Belgium) for kind supplying the phenalkamine curing agent.

Literature

[1] M. Kozako, H. Nakatsu, H. Toda, S. Yamada, K. Yoshinaga, M. Hikita, D. Hirata, T. Miyamoto, M. Takei, Basic investigation of epoxy resin coatings with dispersed carbon nanotubes, Electron. Comm. Jpn. 97 (2014) 24–32. doi:10.1002/ecj.11555.

[2] M. Martin-Gallego, M. Hernández, V. Lorenzo, R. Verdejo, M.A. Lopez-Manchado, M. Sangermano, Cationic photocured epoxy nanocomposites filled with different carbon fillers, Polymer. 53 (2012) 1831–1838. doi:10.1016/j.polymer.2012.02.054.

[3] Y.G. Jeong, J.E. An, Effects of mixed carbon filler composition on electric heating behavior of thermally-cured epoxy-based composite films, Compos. Part A. 56 (2014) 1–7. doi:10.1016/j.compositesa.2013.09.003.

[4] Z.A. Ghaleb, M. Mariatti, Z.M. Ariff, Properties of graphene nanopowder and multi-walled carbon nanotube-filled epoxy thin-film nanocomposites for electronic applications: The effect of sonication time and filler loading, Compos. Part A. 58 (2014) 77–83. doi:10.1016/j.compositesa.2013.12.002.

[5] S. Park, M. Shon, Effects of multi-walled carbon nano tubes on corrosion protection of zinc rich epoxy resin coating, J. Ind. Eng. Chem. 21 (2015) 1258–1264. doi:10.1016/j.jiec.2014.05.042.

[6] S. Kugler, K. Kowalczyk, T. Spychaj, Hybrid carbon nanotubes/graphene modified acrylic coats, Prog. Org. Coat. 85 (2015) 1–7. doi:10.1016/j.porgcoat.2015.02.019.

[7] M. Sangermano, E. Borella, A. Priola, M. Messori, R. Taurino, P. Pötschke, Use of single-walled carbon nanotubes as reinforcing fillers in UV-curable epoxy systems, Macromol. Mater. Eng. 293 (2008) 708–713. doi:10.1002/mame.200800126.
[8] M. Sangermano, S. Pegel, P. Pötschke, B. Voit, Antistatic epoxy coatings with carbon nanotubes obtained by cationic photopolymerization, Macromol. Rapid Commun. 29 (2008) 396–400. doi:10.1002/marc.200700720.
[9] S. Kugler, T. Spychaj, Carbon nanostructures and films or coatings based on them. Part II. Films and polymer coatings with carbon nanostructures, Polimery (Warsaw). 58 (2013) 177–180. doi:10.14314/polimery.2013.177.
[10] S. Kugler, K. Kowalczyk, T. Spychaj, Influence of dielectric nanoparticles addition on electroconductivity and other properties of carbon nanotubes-based acrylic coatings, Prog. Org. Coat. 92 (2016) 66–72. doi:10.1016/j.porgcoat.2015.12.006.
[11] K. Kowalczyk, S. Kugler, T. Spychaj, Antistatic polyurethane coats with hybrid carbon nanofillers, Polimery (Warsaw). 59 (2014) 650–655. doi:10.14314/polimery.2014.650.
[12] A. Gergely, Z. Pászti, J. Mihály, E. Drotár, T. Török, Galvanic function of zinc-rich coatings facilitated by percolating structure of the carbon nanotubes. Part II: Protection properties and mechanism of the hybrid coatings, Prog. Org. Coat. 77 (2014) 412–424. doi:10.1016/j.porgcoat.2013.11.004.
[13] L. Diblíková, A. Koukalová, J. Kudláček, M. Zoubek, F. Herrmann, Properties of functional epoxy coatings modified by carbon nanoparticles, Sol. St. Phen. 227 (2015) 127–130. doi:10.4028/www.scientific.net/SSP.227.127.
[14] Y. He, C. Chen, F. Zhong, H. Chen, D. Qing, Synthesis and properties of iron oxide coated carbon nanotubes hybrid materials and their use in epoxy coatings, Polym. Adv. Technol. 26 (2015) 414–421. doi:10.1002/pat.3470.
[15] A. Kalendová, D. Veselý, M. Kohl, J. Stejskal, Anticorrosion efficiency of zinc-filled epoxy coatings containing conducting polymers and pigments, Prog. Org. Coat. 78 (2015) 1–20. doi:10.1016/j.porgcoat.2014.10.009.
[16] G.V. Pham, A.T. Trinh, T.X.H. To, T.D. Nguyen, T.T. Nguyen, X.H. Nguyen, Incorporation of Fe3O4/CNTs nanocomposite in an epoxy coating for corrosion protection of carbon steel, Adv. Nat. Sci: Nanosci. Nanotechnol. 5 (2014) 35016. doi:10.1088/2043-6262/5/3/035016.
[17] P. Deshpande, S. Vathare, S. Vagge, E. Tomšík, J. Stejskal, Conducting polyaniline/multi-wall carbon nanotubes composite paints on low carbon steel for corrosion protection: electrochemical investigations, Chem. Pap. 67 (2013) 1072–1078. doi:10.2478/s11696-012-0273-9.
[18] H. Jeon, J. Park, M. Shon, Corrosion protection by epoxy coating containing multi-walled carbon nanotubes, J. Ind. Eng. Chem. 19 (2013) 849–853. doi:10.1016/j.jiec.2012.10.030.
[19] Z. Zhang, W. Zhang, D. Li, Y. Sun, Z. Wang, C. Hou, L. Chen, Y. Cao, Y. Liu, Mechanical and anticorrosive properties of graphene/epoxy resin composites coating prepared by in-situ method, Int. J. Mol. Sci. 16 (2015) 2239–2251. doi:10.3390/ijms16012239.
[20] V. Patil, R.V. Dennis, T.K. Rout, S. Banerjee, G.D. Yadav, Graphene oxide and functionalized multi walled carbon nanotubes as epoxy curing agents: a novel synthetic approach to nanocomposites containing active nanostructured fillers, RSC Adv. 4 (2014) 49264–49272. doi:10.1039/C4RA09693B.
[21] Y. He, Y. Fan, C. Chen, F. Zhong, D. Qing, Synthesis of mica-multiwalled carbon nanotube (MWCNT) hybrid material and properties of mica-MWCNT/epoxy composites coating research, High Perform. Polym. 27 (2015) 191–199. doi:10.1177/0954008314542475.

[22] Y. He, C. Chen, F. Zhong, H. Chen, Synthesis and characterization: silicon oxide-coated multiwalled carbon nanotubes and properties of composite coating research, High Perform. Polym. 27 (2015) 352–361. doi:10.1177/0954008314551033.
[23] R.B. Naik, S.B. Jagtap, D. Ratna, Effect of carbon nanofillers on anticorrosive and physico-mechanical properties of hyperbranched urethane alkyd coatings, Prog. Org. Coat. 87 (2015) 28–35. doi:10.1016/j.porgcoat.2015.05.001.
[24] R.B. Naik, S.B. Jagtap, R.S. Naik, N.G. Malvankar, D. Ratna, Effect of non-ionic surfactants on thermomechanical properties of epoxy/multiwall carbon nanotubes composites, Prog. Org. Coat. 77 (2014) 1883–1889. doi:10.1016/j.porgcoat.2014.06.024.
[25] N.W. Khun, B.C.R. Troconis, G.S. Frankel, Effects of carbon nanotube content on adhesion strength and wear and corrosion resistance of epoxy composite coatings on AA2024-T3, Prog. Org. Coat. 77 (2014) 72–80. doi:10.1016/j.porgcoat.2013.08.003.
[26] L.H. Esposito, J.A. Ramos, G. Kortaberria, Dispersion of carbon nanotubes in nanostructured epoxy systems for coating application, Prog. Org. Coat. 77 (2014) 1452–1458. doi:10.1016/j.porgcoat.2014.05.001.
[27] M. Barletta, S. Vesco, M. Puopolo, V. Tagliaferri, High performance composite coatings on plastics: UV-curable cycloaliphatic epoxy resins reinforced by graphene or graphene derivatives, Surf. Coat. Technol. 272 (2015) 322–336. doi:10.1016/j.surfcoat.2015.03.046.
[28] P. Król, B. Król, K. Pielichowska, M. Špírková, Composites prepared from the waterborne polyurethane cationomers—modified graphene. Part I. Synthesis, structure, and physicochemical properties, Colloid Polym. Sci. 293 (2014) 421–431. doi:10.1007/s00396-014-3417-3.
[29] M. Martin-Gallego, R. Verdejo, M.A. Lopez-Manchado, M. Sangermano, Epoxy-Graphene UV-cured nanocomposites, Polymer. 52 (2011) 4664–4669. doi:10.1016/j.polymer.2011.08.039.
[30] S. Liu, C. Wang, Z. Wei, W. Lv, S. Fan, S. Zhu, F. Wang, One-step surface modification of multi-walled carbon nanotubes by pyrrole, Mater. Lett. 134 (2014) 91–94. doi:10.1016/j.matlet.2014.07.011.
[31] N.A. Siddiqui, M.-L. Sham, B.Z. Tang, A. Munir, J.-K. Kim, Tensile strength of glass fibres with carbon nanotube–epoxy nanocomposite coating, Compos. Part A. 40 (2009) 1606–1614. doi:10.1016/j.compositesa.2009.07.005.
[32] S. Kugler, T. Spychaj, Carbon nanostructures and films or coatings based on them. Part I. General characteristics, functionalization and methods of research of compositions containing nanotubes or graphenes, Polimery (Warsaw). 58 (2013) 93–99. doi:10.14314/polimery.2013.093.
[33] L.M. Chiacchiarelli, M. Rallini, M. Monti, D. Puglia, J.M. Kenny, L. Torre, The role of irreversible and reversible phenomena in the piezoresistive behavior of graphene epoxy nanocomposites applied to structural health monitoring, Compos. Sci. Technol. 80 (2013) 73–79. doi:10.1016/j.compscitech.2013.03.009.
[34] B. Marinho, M. Ghislandi, E. Tkalya, C.E. Koning, G. de With, Electrical conductivity of compacts of graphene, multi-wall carbon nanotubes, carbon black, and graphite powder, Powder Technol. 221 (2012) 351–358. doi:10.1016/j.powtec.2012.01.024.
[35] B.L. Burton, Amine-blushing problems? No sweat!, Huntsman Corp., Epoxy Resin Formulators' meeting, The Society of the Plastics Industry, fall 2001. (n.d.). Huntsman Corp., Epoxy Resin Formulators' meeting, The Society of the Plastics Industry, fall 2001.
[36] Amine applications and properties data, Technical bulletin, Huntsman.
[37] SIDS Initial Assessment Report for SIAM 18 (3-Aminomethyl-3,5,5-trimethylcyclohexylamine), UNEP Publications, Paris 2004.

[38] SIDS Initial Assessment Report for SIAM 13 (1,3-Bis(aminomethyl)benzene), UNEP Publications, Bern 2001.
[39] P. Czub, Z. Bończa-Tomaszewski, P. Penczek, J. Pielichowski, Chemistry and technology of epoxy resins, WNT, Warszawa, 2002.
[40] L. Vertuccio, S. Russo, M. Raimondo, K. Lafdi, L. Guadagno, Influence of carbon nanofillers on the curing kinetics of epoxy-amine resin, RSC Adv. 5 (2015) 90437–90450. doi:10.1039/C5RA14343H.
[41] American National Standard Institute (ANSI/ESD) S541, (2003).
[42] J. Liu, R. Liu, Y. Yuan, S. Zhang, X. Liu, Preparation of superhydrophobic antistatic coatings from branched alternating copolymers P(St-alt-MAn) and carbon nanotubes based on organic–inorganic hybrid approach, Prog. Org. Coat. 76 (2013) 1251–1257. doi:10.1016/j.porgcoat.2013.03.022.
[43] H. Ha, S.C. Kim, K. Ha, UV curing kinetics and properties of polyurethane acrylate/multi-walled carbon nanotube coatings, Macromol. Res. 18 (2010) 674–679. doi:10.1007/s13233-010-0705-8.

FIGURES

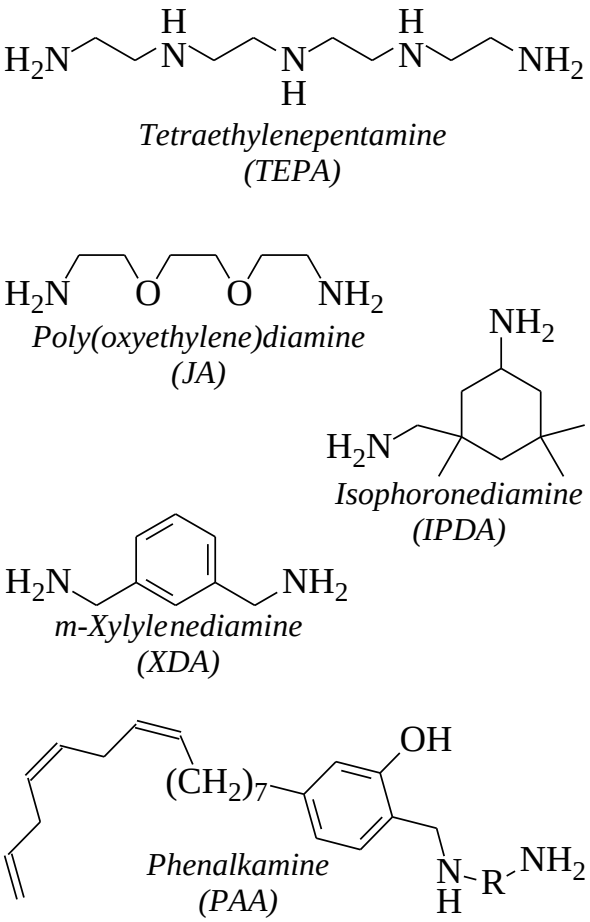

Fig. 1. Chemical structures of tested amines.

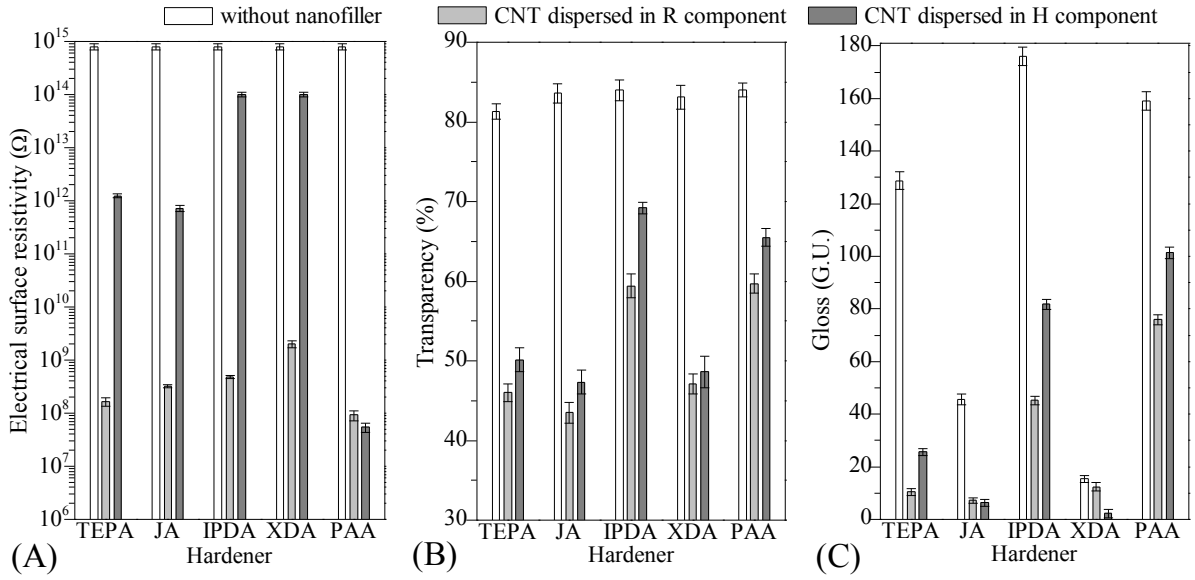

Fig. 2. Electrical surface resistivity (A), transparency (B) and gloss (C) of epoxy coatings (unfilled or containing 0.35 wt.% of CNT).

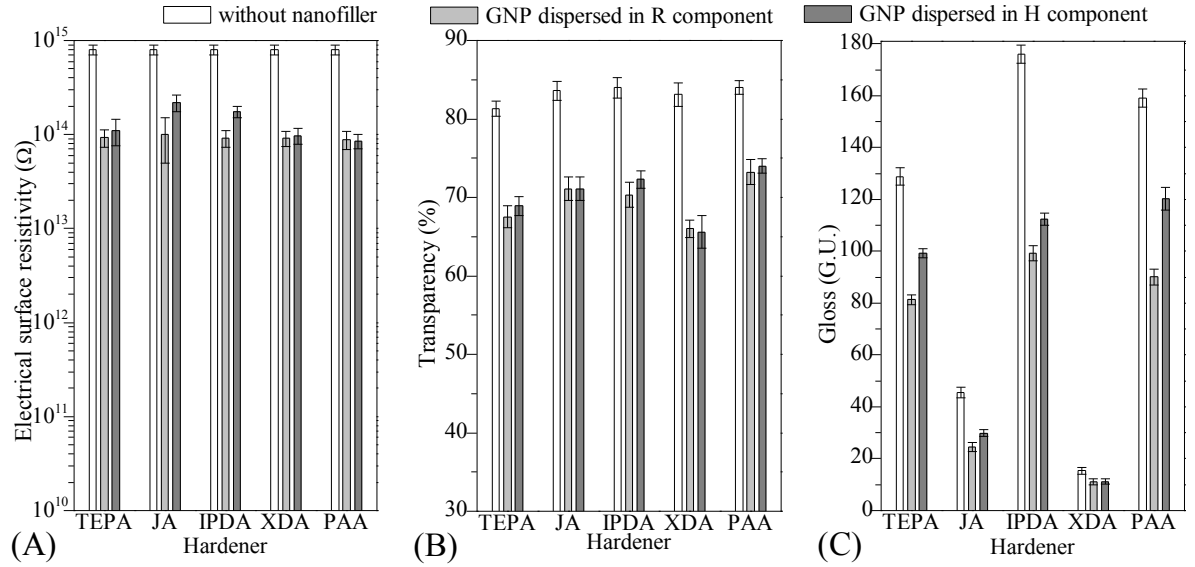

Fig. 3. Electrical surface resistivity (A), transparency (B) and gloss (C) of epoxy coatings (unfilled or containing 0.35 wt.% of GNP)

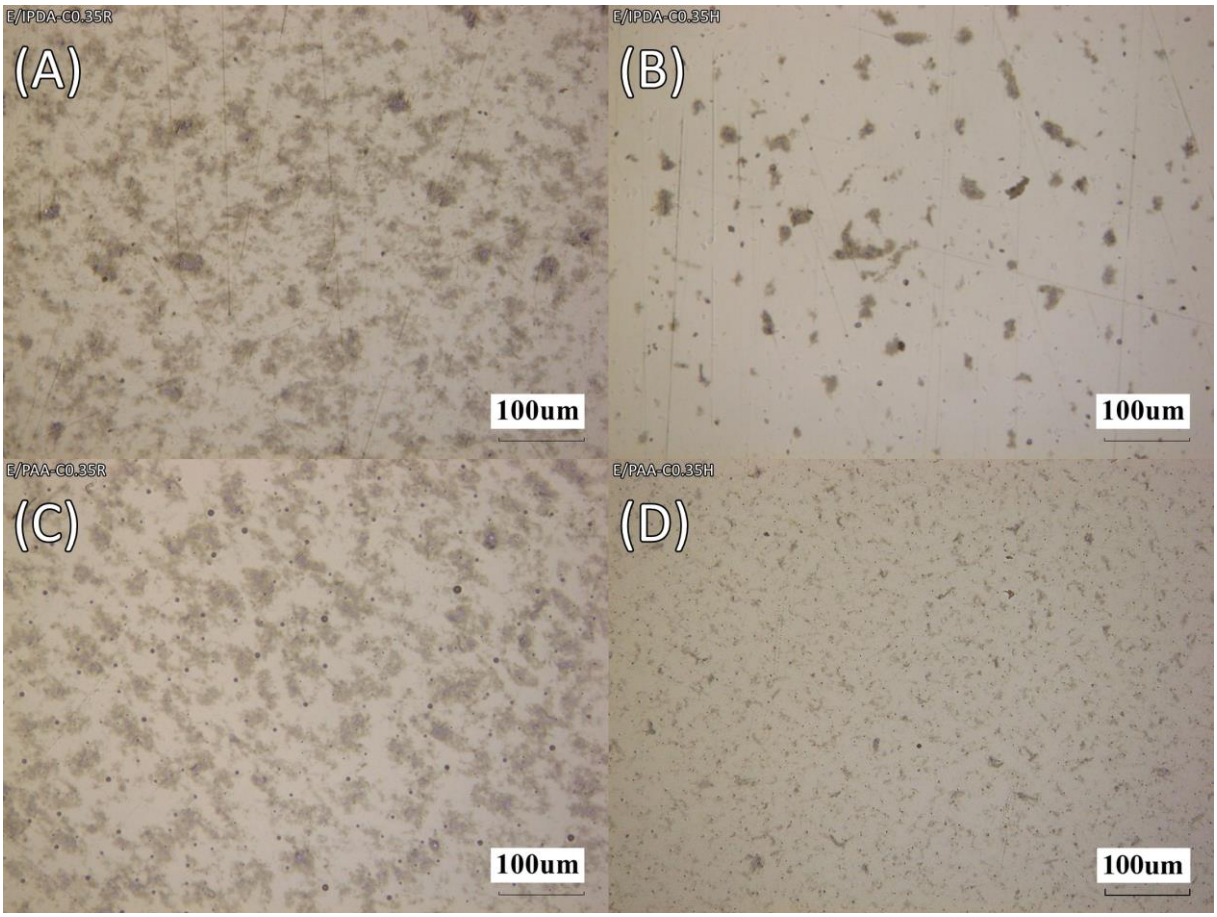

Fig. 4. Microphotographs of epoxy coatings containing 0.35 wt.% of CNT: (A) E/IPDA-C0.35R, (B) E/IPDA-C0.35H, (C) E/PAA-C0.35R and (D) E/PAA-C0.35H.

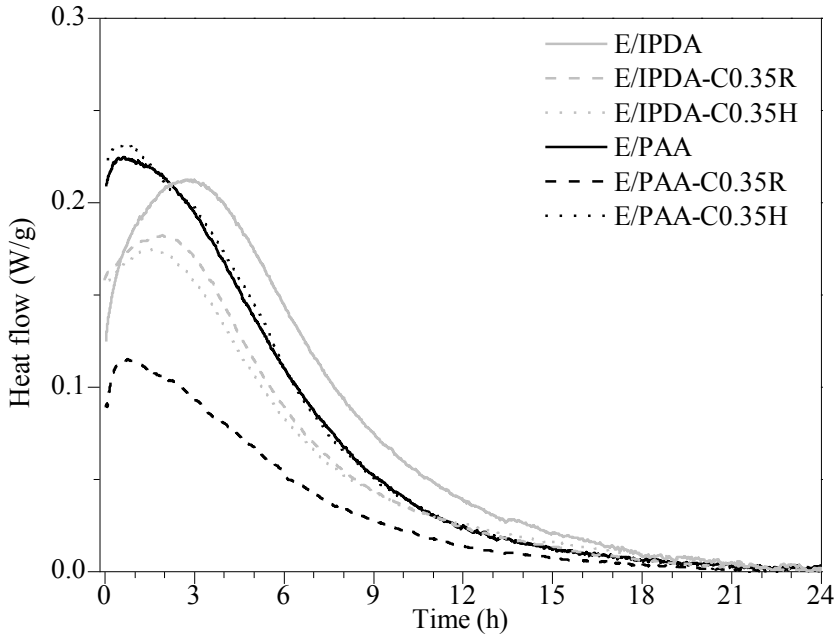

Fig. 5. DSC thermographs for epoxy coating compositions (isothermal curing process for 24h)

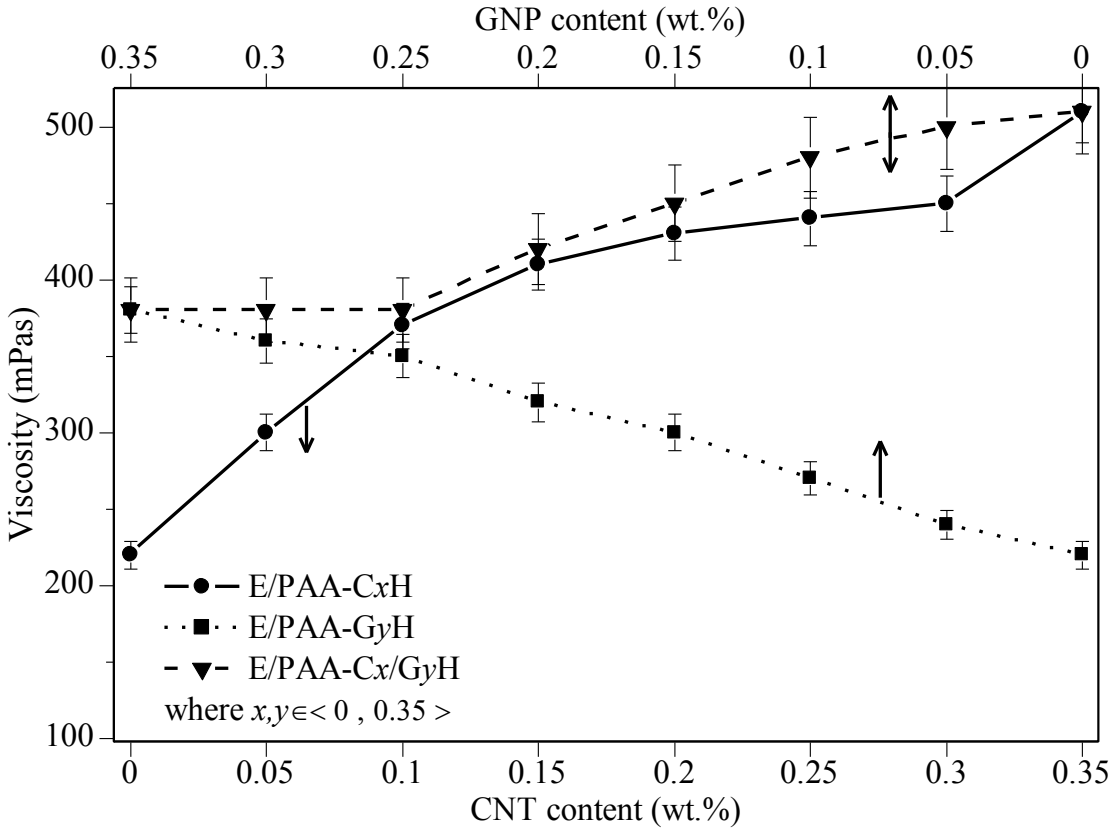

Fig. 6. Viscosity of epoxy varnishes based on carbon nanofillers predispersed in PAA hardener.

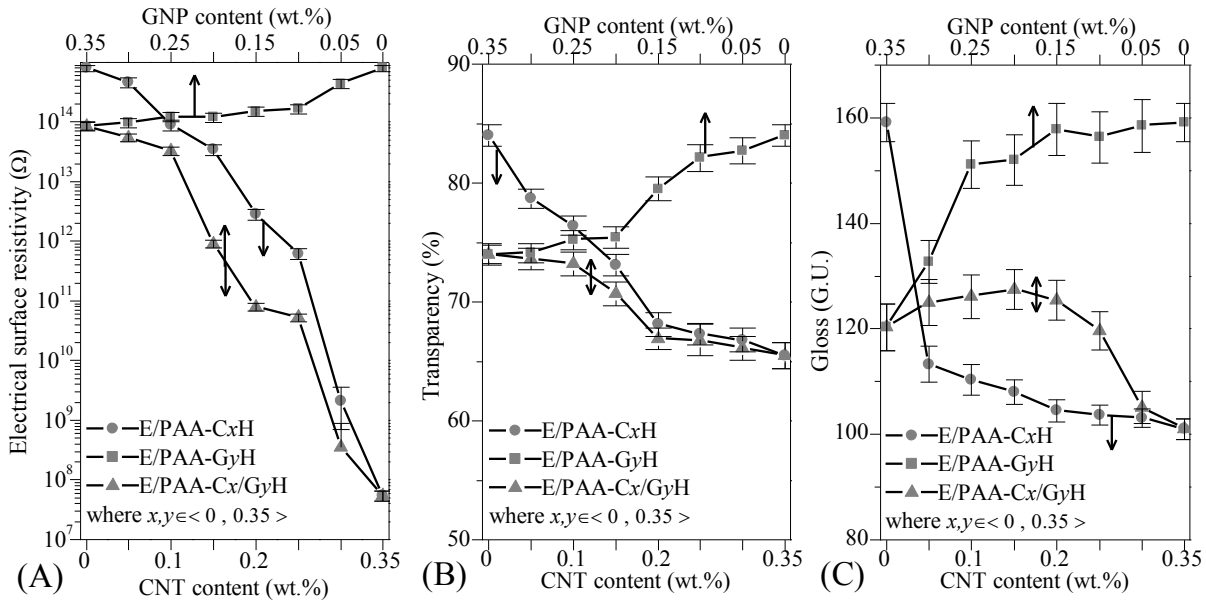

Fig. 7. Electrical surface resistivity (A), transparency (B) and gloss (C) of epoxy coatings based on carbon nanofillers predispersed in PAA hardener.

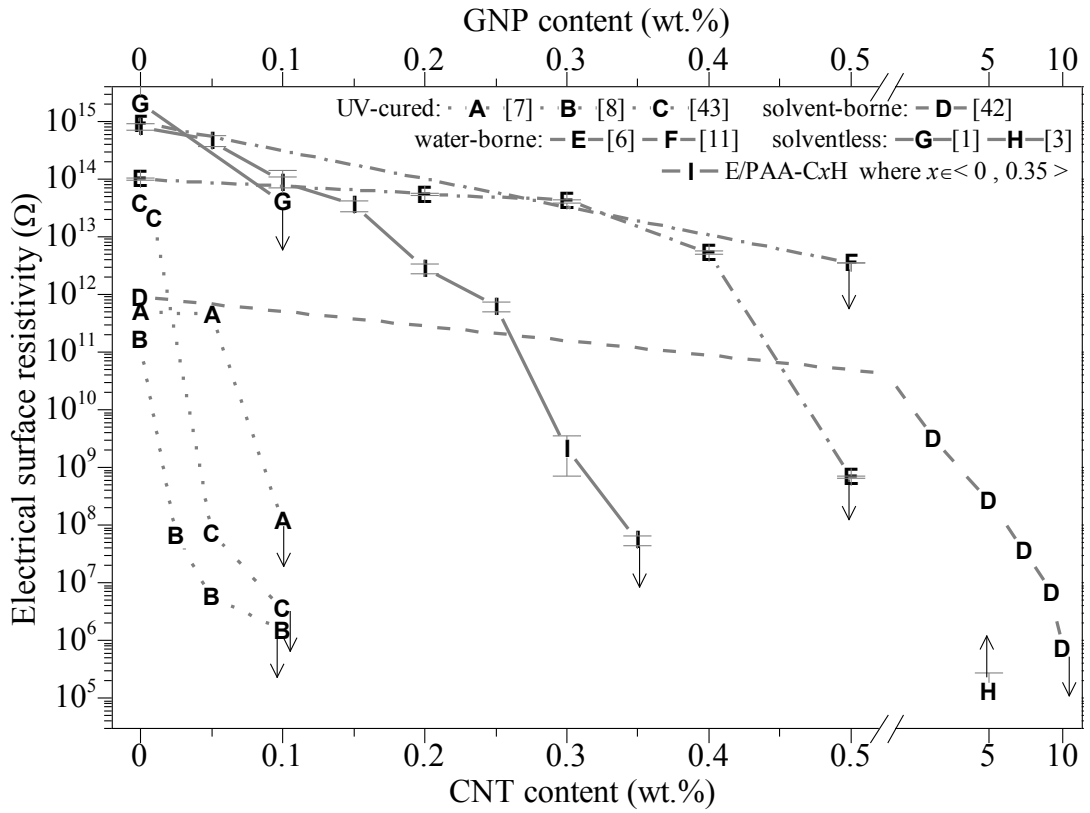

Fig. 8. Electrical surface resistivity values for epoxy coatings (based on CNT predispersed in PAA hardener) and coatings presented in a literature.

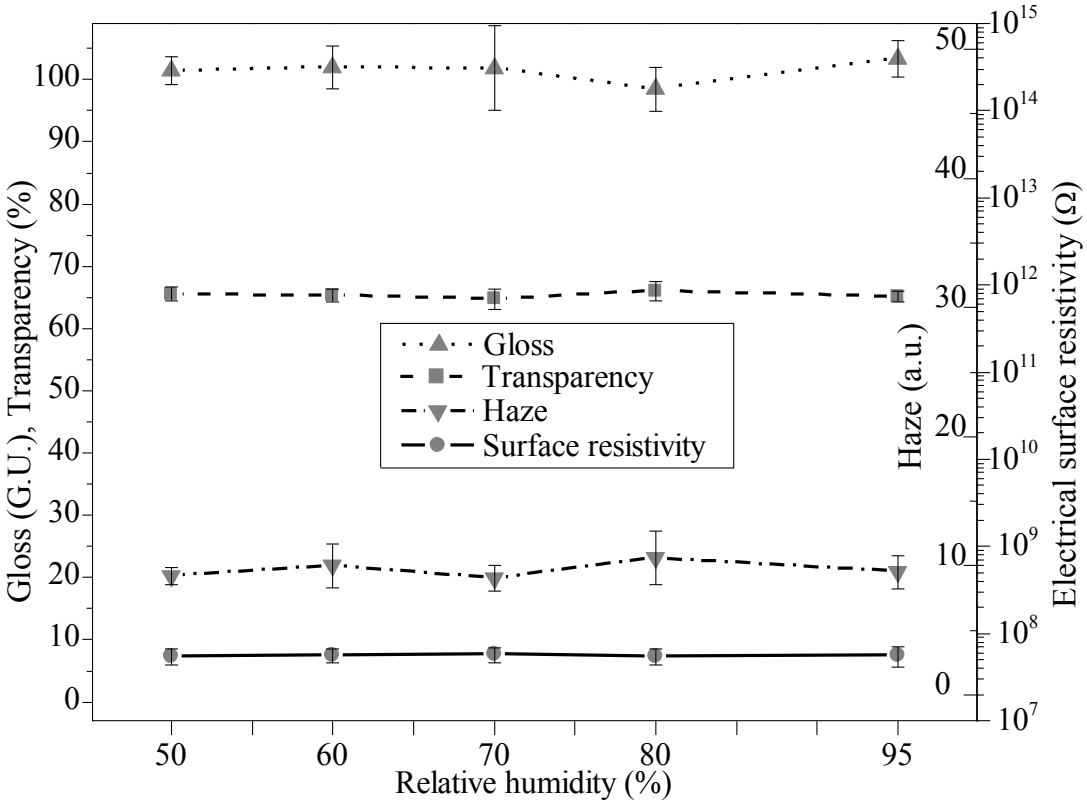

Fig. 9. Gloss, transparency, electrical surface resistivity and haze values for E/PAA-C0.35H coatings (stored at various humidity).

TABLES

Table 1. Characteristics of epoxy coatings with carbon nanofillers.

Sample acronym	Nanofiller content[a]		Curing agent	Carbon nanofiller dispersing medium	Surface resistivity (Ω)	T_g [d] (°C)
	CNT	GNP				
E/TEPA	0	0	TEPA	–	$1.0 \cdot 10^{15}$	60
E/TEPA-C0.35R	0.35	0		R [b]	$1.7 \cdot 10^{8}$	58
E/TEPA-C0.35H				H [c]	$1.2 \cdot 10^{12}$	65
E/TEPA-G0.35R	0	0.35		R	$9.3 \cdot 10^{13}$	— [e]
E/TEPA-G0.35H				H	$1.1 \cdot 10^{14}$	—
E/JA	0	0	JA	–	$1.0 \cdot 10^{15}$	53
E/JA-C0.35R	0.35	0		R	$3.2 \cdot 10^{8}$	53
E/JA-C0.35H				H	$7.2 \cdot 10^{11}$	56
E/JA-G0.35R	0	0.35		R	$1.0 \cdot 10^{14}$	—
E/JA-G0.35H				H	$2.2 \cdot 10^{14}$	—
E/IPDA	0	0	IPDA	–	$1.0 \cdot 10^{15}$	68
E/IPDA-C0.35R	0.35	0		R	$4.8 \cdot 10^{8}$	66
E/IPDA-C0.35H				H	$1.1 \cdot 10^{14}$	68
E/IPDA-G0.35R	0	0.35		R	$9.2 \cdot 10^{13}$	—
E/IPDA-G0.35H				H	$1.8 \cdot 10^{14}$	—
E/XDA	0	0	XDA	–	$1.0 \cdot 10^{15}$	52
E/XDA-C0.35R	0.35	0		R	$2.0 \cdot 10^{9}$	50
E/XDA-C0.35H				H	$1.2 \cdot 10^{14}$	52
E/XDA-G0.35R	0	0.35		R	$9.1 \cdot 10^{13}$	—
E/XDA-G0.35H				H	$9.7 \cdot 10^{13}$	—
E/PAA	0	0	PAA	–	$1.0 \cdot 10^{15}$	22
E/PAA-C0.05H	0.05	0		H	$4.6 \cdot 10^{14}$	—
E/PAA-C0.1H	0.1				$8.9 \cdot 10^{13}$	—
E/PAA-C0.15H	0.15				$3.4 \cdot 10^{13}$	—
E/PAA-C0.2H	0.2				$2.9 \cdot 10^{12}$	23
E/PAA-C0.25H	0.25				$6.2 \cdot 10^{11}$	—
E/PAA-C0.3H	0.3				$2.1 \cdot 10^{9}$	—
E/PAA-C0.35H	0.35				$5.5 \cdot 10^{7}$	29
E/PAA-C0.35R				R	$9.2 \cdot 10^{7}$	29
E/PAA-C0.3/G0.05H	0.3	0.05		H	$3.5 \cdot 10^{8}$	—
E/PAA-C0.25/G0.1H	0.25	0.1			$5.3 \cdot 10^{10}$	—
E/PAA-C0.2/G0.15H	0.2	0.15			$8.0 \cdot 10^{10}$	23
E/PAA-C0.15/G0.2H	0.15	0.2			$9.0 \cdot 10^{11}$	—
E/PAA-C0.1/G0.25H	0.1	0.25			$3.3 \cdot 10^{13}$	—
E/PAA-C0.05/G0.3H	0.05	0.3			$5.5 \cdot 10^{13}$	—
E/PAA-G0.35H	0	0.35			$8.6 \cdot 10^{13}$	22
E/PAA-G0.35R				R	$8.9 \cdot 10^{13}$	—
E/PAA-G0.3H		0.3		H	$1.0 \cdot 10^{14}$	
E/PAA-G0.25H		0.25			$1.2 \cdot 10^{14}$	—
E/PAA-G0.2H		0.2			$1.2 \cdot 10^{14}$	—
E/PAA-G0.15H		0.15			$1.5 \cdot 10^{14}$	22
E/PAA-G0.1H		0.1			$1.7 \cdot 10^{14}$	—
E/PAA-G0.05H		0.05		R	$4.4 \cdot 10^{14}$	—

a – nanofiller content in a dry coat (wt. %); b – the resinous component containing DGEBF and CGE
c – the hardener component containing a curing agent and reactive plasticizer; d – glass transition temperature (DSC technique); e – not tested

Table 2. Characteristics of epoxy compositions curing process.

Sample acronym	Nanofiller content[a]		t_{max}[b] (min)	α_{Hmax}[c] (%)	ΔH_{cure}[d] (J/g)	$t_{\alpha 1/2}$[e] (min)
	CNT	GNP				
E/TEPA	0	0	70	19	507	165
E/JA			131	26	320	224
E/XDA			215	55	365	213
E/IPDA			184	34	309	283
E/IPDA-C0.35R	0.35	0	127	27 (23[f])	258	234 (348[f])
E/IPDA-C0.35H			99	21 (13)	188	242 (381)
E/PAA	0	0	49	6	304	232
E/PAA-C0.35R	0.35	0	57	14 (7)	143	233 (1305)
E/PAA-C0.35H			49	10 (10)	305	228 (233)
E/PAA-G0.35R	0	0.35	35	6 (4)	179	249 (464)
E/PAA-G0.35H			23	5 (5)	300	210 (222)

a – nanofiller content in a dry coat (wt. %); b – time to maximum heat flow; c – epoxy groups conversion at a heat flow peak; d – total enthalpy of the curing process; e – time to 50% conversion of epoxy groups; f – in relation to ΔH_{cure} of the unfilled composition (E/IPDA or E/PAA)

Table 3. Mechanical and thermal features of epoxy coatings based on PAA.

Sample acronym	Hardness (a.u.)	Cupping resistance (mm)	Adhesion [a] (°)	T_{10}[b] (°C)
E/PAA	147 ± 4	10.0 ± 0.1	0	309
E/PAA-C0.2H	144 ± 3	11.6 ± 0.1	0	292
E/PAA-C0.35H	145 ± 3	12.0 ± 0.1	0	294
E/PAA-C0.2/G0.15H	143 ± 4	11.6 ± 0.1	0	301
E/PAA-G0.35H	141 ± 3	11.3 ± 0.2	0	310
E/PAA-G0.15H	141 ± 3	11.1 ± 0.1	0	300

a – rating scale 0-5 (0 – the best, 5 – the worst); b – temperature at 10% mass loss